

# *Robustness of serial clustering of extratropical cyclones to the choice of tracking method*

Article

Accepted Version

Pinto, J. G., Ulbrich, S., Economou, T., Stephenson, D. B., Karremann, M. K. and Shaffrey, L. C. ORCID: <https://orcid.org/0000-0003-2696-752X> (2016) Robustness of serial clustering of extratropical cyclones to the choice of tracking method. *Tellus A*, 68. 32204. ISSN 1600-0870 doi: <https://doi.org/10.3402/tellusa.v68.32204> Available at <https://centaur.reading.ac.uk/66165/>

It is advisable to refer to the publisher's version if you intend to cite from the work. See [Guidance on citing](#).

To link to this article DOI: <http://dx.doi.org/10.3402/tellusa.v68.32204>

Publisher: Co-Action Publishing

All outputs in CentAUR are protected by Intellectual Property Rights law, including copyright law. Copyright and IPR is retained by the creators or other copyright holders. Terms and conditions for use of this material are defined in the [End User Agreement](#).

[www.reading.ac.uk/centaur](http://www.reading.ac.uk/centaur)

**CentAUR**

Central Archive at the University of Reading

Reading's research outputs online

1 **Robustness of serial clustering of extra-tropical cyclones to**  
2 **the choice of tracking method**

3  
4 Joaquim G. Pinto\*

5 Department of Meteorology, University of Reading, UK and  
6 Institute for Geophysics and Meteorology, University of Cologne, Germany

7  
8 Sven Ulbrich

9 Institute for Geophysics and Meteorology, University of Cologne, Germany

10 Theodoros Economou, David B. Stephenson,

11 Department of Mathematics, University of Exeter, UK

12 Melanie K. Karremann

13 Karlsruhe Institute of Technology, Institute of Meteorology and Climate Research, Germany

14 Len C. Shaffrey

15 NCAS-Climate, Department of Meteorology, University of Reading, UK

16  
17  
18 Tellus A - Thematic Cluster

19 “Intercomparison of Mid-Latitude Storm Diagnostics”

20  
21 Accepted version 4 July 2016

22 doi:10.3402/tellusa.v68.32204

---

\*Corresponding author address: Joaquim G. Pinto, Department of Meteorology, University of Reading, Earley Gate, PO Box 243, Reading RG6 6BB, United Kingdom  
E-mail: j.g.pinto@reading.ac.uk

23 **Abstract**

24 Cyclone clusters are a frequent synoptic feature in the Euro-Atlantic area. Recent studies have  
25 shown that serial clustering of cyclones generally occurs on both flanks and downstream  
26 regions of the North Atlantic storm track, while cyclones tend to occur more regularly on the  
27 eastern side of the North Atlantic basin near Newfoundland. This study explores the  
28 sensitivity of serial clustering to the choice of cyclone tracking method using cyclone track  
29 data from 15 methods derived from ERA-Interim data (1979-2010). Clustering is estimated by  
30 the dispersion (ratio of variance to mean) of winter (DJF) cyclone passages near each grid  
31 point over the Euro-Atlantic area. The mean number of cyclone counts and their variance are  
32 compared between methods, revealing considerable differences, particularly for the latter.  
33 Results show that all different tracking methods qualitatively capture similar large-scale  
34 spatial patterns of underdispersion / overdispersion over the study region. The quantitative  
35 differences can primarily be attributed to the differences in the variance of cyclone counts  
36 between the methods. Nevertheless, overdispersion is statistically significant for almost all  
37 methods over parts of the Eastern North Atlantic and Western Europe, and is therefore  
38 considered as a robust feature. The influence of the North Atlantic Oscillation on cyclone  
39 clustering displays a similar pattern for all tracking methods, with one maximum near Iceland  
40 and another between the Azores and Iberia. The differences in variance between methods are  
41 not related with different sensitivities to the NAO, which can account to over 50% of the  
42 clustering in some regions. We conclude that the general features of underdispersion /  
43 overdispersion of extra-tropical cyclones over the North Atlantic and Western Europe is  
44 robust to the choice of tracking method. The same is true for the influence of the North  
45 Atlantic Oscillation on cyclone dispersion.

46 *Keywords:* Poisson process; extra-tropical cyclones, clustering, dispersion statistics, North  
47 Atlantic, Europe, IMILAST, reanalysis.

## 48 **1. Introduction**

49 Extra-tropical cyclones over the North Atlantic play a key role in determining the weather and  
50 climate of Western Europe. Cyclones have a tendency to serially cluster close to Europe  
51 (Mailer et al., 2006), particularly extreme ones (Vitolo et al., 2009; Pinto et al., 2013), which  
52 can lead to severe socio-economic impacts and cumulative losses. A recent example is the  
53 unusually large number of storms that affected the British Isles during the winter of 2013/2014  
54 (Matthews et al., 2014). The winter of 2013/2014 was characterized by exceptionally wet and  
55 windy conditions in this region, and the resulting wind damage and widespread coastal and  
56 inland flooding had a considerable impact on infrastructure and transportation (Huntingford et  
57 al., 2014). Such stormy winters are characterized by the frequent occurrence of cyclone  
58 families (Bjerknes and Solberg, 1922).

59 Pinto et al. (2014) recently provided evidence that the occurrence of cyclone clusters is  
60 governed by a persistent, zonally orientated and extended eddy-driven polar jet stream over  
61 the Eastern North Atlantic and Western Europe, which drives the North Atlantic cyclones  
62 towards the British Isles and sometimes further into Central Europe. The maintenance of these  
63 large-scale conditions is supported by two-sided Rossby wave breaking over the North  
64 Atlantic (Hanley and Caballero, 2012; Gómara et al, 2014; Messori and Caballero, 2015).  
65 Pinto et al. (2014) demonstrated for four selected stormy periods 1990, 1993, 1999 and 2007,  
66 that secondary cyclogenesis (new storms develop on the trailing fronts of previous storms, cf.  
67 Parker, 1998) further contributes to the occurrence of cyclones clusters arriving into Western  
68 Europe in rapid succession.

69 If cyclone occurrences at a certain area were completely random, then they can be statistically  
70 modelled as Poisson (point) process. Deviations from a Poisson process can indicate whether  
71 cyclones occur either in a more clustered (cyclones occur in groups) or a more regular way  
72 (time between occurrences almost constant). Thus, implementing Poisson models to cyclone

73 count data can be used as a way of quantifying the amount of clustering/regularity (e.g.,  
74 Mailier et al., 2006; Vitolo et al., 2009; Pinto et al., 2013; Blender et al., 2015; Economou et  
75 al., 2015). The common result from these publications is that cyclone clustering  
76 (overdispersion) occurs on both flanks and downstream of the North Atlantic storm track  
77 (Mailier et al., 2006, their Fig. 6), while regularity (underdispersion) is found near the core of  
78 the storm track by Newfoundland. This pattern is a robust feature in different reanalysis  
79 datasets (Pinto et al., 2013, their Fig. 3). Global circulation models also broadly capture this  
80 spatial pattern of overdispersion / underdispersion over the North Atlantic and Western  
81 Europe (Economou et al., 2015, their Fig. 2).

82 Previous studies (Mailier et al., 2006; Vitolo et al., 2009) have shown that large-scale  
83 atmospheric modes of variability such as the North Atlantic Oscillation (NAO, e.g. Hurrell et  
84 al., 2003) have a strong influence on cyclone clustering. The NAO is the dominant large-scale  
85 atmospheric pattern over the North Atlantic and Western Europe. The NAO has two centers of  
86 action, the Azores high and the Icelandic low, and its index is a proxy for the strength of the  
87 westerlies over the Northeast Atlantic. Thus, the NAO largely determines the weather  
88 conditions over this area, particularly in wintertime. The NAO varies on time scales ranging  
89 from days to centuries, but with dominant interdecadal to decadal time scales (Pinto and  
90 Raible, 2012). Cyclone tracks are shifted northward and extended downstream in positive  
91 NAO phases, while they are shorter and shifted southward in negative NAO phases (e.g.,  
92 Pinto et al., 2009). Furthermore, the NAO and other large-scale modes affect both the  
93 frequency and intensity of extratropical cyclones over the North Atlantic (Hunter et al., 2016).  
94 The existence of clustering has been associated with NAO variability (e.g. Mailier et al.,  
95 2006), as a prolonged time period with a dominant NAO phase will tend to direct cyclones  
96 over the North Atlantic towards a specific area (Pinto et al., 2009), thus enhancing (reducing)  
97 the number of cyclone counts in that specific area (other areas). Simple models have been

98 developed to analyse the relationship between NAO and cyclone activity, revealing that a  
99 considerable part of the clustering is related to NAO variability (e.g. Mailier et al., 2006;  
100 Vitolo et al., 2009; Economou et al., 2015). This is true for both reanalysis datasets and global  
101 climate models.

102 Publications quantifying cyclone clustering over the North Atlantic have used single cyclone  
103 tracking methods, either Hodges (1994), Murray and Simmonds (1991) or Blender et al.  
104 (1997). As noted by Neu (2013), there is no single scientific definition of what an extratropical  
105 cyclone is, and thus no consensus on the best atmospheric variable to use, leading to different  
106 approaches for identifying and tracking cyclones. As a consequence, cyclone statistics and  
107 characteristics differ depending on the cyclone tracking method and/or the key variable used  
108 (e.g., Hoskins and Hodges, 2002; Raible et al., 2008; Rudeva et al., 2014). One of the  
109 objectives of the Intercomparison of Mid-Latitude Storm Diagnostics (IMILAST) project is to  
110 understand which cyclone statistics are robust to the choice of tracking algorithm (Neu et al.,  
111 2013). Such an assessment is necessary to be able to provide objective information to  
112 stakeholders regarding cyclone activity in general and windstorms in particular (Hewson and  
113 Neu, 2015).

114 The present manuscript is a contribution to the IMILAST project. The main question explored  
115 in this study is how robust the general features of underdispersion / overdispersion over the  
116 study area are to the choice of cyclone tracking method. With this aim, we perform for the first  
117 time a multi-tracking approach analysis of clustering over the North Atlantic and Europe. The  
118 second aim is to evaluate how the NAO influence on cyclone clustering depends on the choice  
119 of tracking method. Section 2 describes the datasets and methodologies used. The  
120 quantification of cyclone passages is explained in section 3, together with a description of  
121 mean and variance of counts. Section 4 presents the clustering as identified for all the 15

122 methods and investigates spread between methods. Section 5 quantifies the links between  
123 clustering and the NAO variability. A short conclusion follows.

124

## 125 **2. Data and Methods**

### 126 *The IMILAST project cyclone track dataset*

127 One of the main objectives of the IMILAST project is to document and understand the  
128 sensitivity of the representation of cyclone activity and extreme windstorms in reanalysis  
129 datasets and global climate model simulations to the choice of cyclones tracking method. In  
130 particular, the IMILAST team has been evaluating which cyclone features are largely  
131 independent of the tracking method used (and hence can be regarded as robust), and which  
132 features differ between tracking methods. In a first analysis, Neu et al. (2013) concluded that  
133 differences between methods are typically small for long-lived, transient, deep, intense lows  
134 over large oceanic basins. This is not unexpected, as extremes associated with extratropical  
135 cyclones (e.g., minimum sea level pressure, vorticity, peak winds) are strongly inter-related  
136 (Economou et al., 2014). On the other hand, considerable discrepancies between tracking  
137 methods are found for short-lived, shallow, and slow moving systems, particularly over areas  
138 like the Mediterranean or over the continents (Neu et al., 2013; Lionello et al., 2016). More  
139 details on the inter-comparison strategy, general results and proposed future directions of  
140 research are discussed in Hewson and Neu (2015).

141 The cyclone track database from the IMILAST project is used here to estimate the dispersion  
142 of cyclone counts over the North Atlantic and Europe. The cyclone tracks were derived with  
143 multiple cyclone tracking methods (see Neu et al., their Table 1) based on European Centre for  
144 Medium-Range Weather Forecasts (ECMWF) Interim Reanalysis (ERA-Interim; Dee et al.,  
145 2011). The horizontal resolution of the dataset is T255 (approximately  $0.75^\circ \times 0.75^\circ$  latitude /  
146 longitude), with 60 vertical levels from surface up to 0.1 hPa. The data was interpolated to



147 1.5°x1.5° and made available to all IMILAST participants. The investigation period is  
148 December 1979 to February 2010 (at 6-hourly resolution), and only winter months are  
149 analysed (December, January, February: DJF). Here, we consider results from 14 tracking  
150 methods from the IMILAST project (cf. Table 1, M02-M22). Additionally, we considered also  
151 cyclone tracks derived with the Hodges tracking method (Hodges, 1994, 1999; Hodges et al.,  
152 2011, HOD) for the same time period and set up as the IMILAST tracking data. Tracks over  
153 high orography (>1500 m) are not considered (e.g. Greenland, Atlas Mountains) and such  
154 areas are disregarded in this study. All tracks have a lifetime of at least 24 hours (five time  
155 frames). For specific details on the individual methods see references inserted in Table 1.  
156 Comparisons between the tracking methods are presented in e.g., Raible et al. (2008), Neu et  
157 al. (2013), Rudeva et al. (2014) and Lionello et al. (2016). Several case studies are discussed  
158 in Hewson and Neu (2015), including comparisons to observations. The colors of the method  
159 in Figures 1 and 5 correspond to the type of method (cf. Table 1): Green colours for 850 hPa  
160 vorticity (M07, M18, M21, HOD), grey for 850 hPa geopotential height minimum contour  
161 (M14), orange/brown for mean sea level (MSLP) minimum (M12, M15, M16, M20), red for  
162 MSLP gradient or minimum contour (M06, M08, M22), and blue for Laplacian of MSLP  
163 (M02, M09, M10).

164

### 165 *Quantification of clustering*

166 The occurrence of random events in time can be represented by the homogeneous Poisson  
167 process (Cox and Isham, 1980). If the events (cyclones) arise with a rate of occurrence  $\lambda$ , then  
168 the number of events  $y$  in a time interval  $T$  is Poisson distributed (random), with mean ( $\bar{y}$ ) and  
169 sample variance ( $s_y^2$ ) both equal to  $\lambda T$ , and thus  $s_y^2 / \bar{y} = 1$ . Deviations from the Poisson  
170 process indicate a non-random arrival of cyclones over time, in the sense that events  
171 systematically occur in a more clustered (in groups) or a more regular way (equal spacing in

172 time; cf. Fig. S1). These deviations from the Poisson process can be used to assess the degree  
173 of clustering, and following Mailier et al. (2006), we use the dispersion statistic:

$$174 \quad \phi = \frac{s_y^2}{\bar{y}} - 1. \quad (1)$$

175 A Poisson process ( $s_y^2 = \bar{y}$ ) with a constant rate of occurrence  $\lambda$  implies  $\phi = 0$ . Positive  
176 values of  $\phi$  indicate clustering (overdispersion;  $s_y^2 > \bar{y}$ ), and negative values of  $\phi$  indicate  
177 regularity (underdispersion;  $s_y^2 < \bar{y}$ ; cf. Fig. S1). Following Pinto et al. (2013), events are  
178 defined as cyclone tracks intercepting a radius of influence around a certain grid point. An  
179 identification radius of 700 km was selected based on considerations related to cyclone sizes  
180 and potential impacts, so the rate is the number of cyclones that pass through this region with  
181 an area of  $\pi \cdot 700\text{km}^2$  (see Pinto et al., 2013 for more details). When a cyclone track intercepts  
182 the circle for a selected grid point, the time corresponding to the nearest position to the circle  
183 center is counted (cf. Fig. 1a for an example). In this way, time series are obtained for each  
184 method (Fig. 1b). This approach is applied at each location (grid point) and was recently used  
185 to estimate clustering of cyclones simulated by CMIP5 global climate models (Economou et  
186 al., 2015). For each winter (DJF), cyclone counts ( $y_i$ ) are computed for the period 1979/80-  
187 2009/10 to produce a time-series of counts  $\{y_1, y_2, \dots, y_n\}$  at each grid point, where  $n$  is the  
188 number of winters.

189

### 190 *Relationship with the North Atlantic Oscillation*

191 As explained in Economou et al. (2015), overdispersion can be approximated by

$$192 \quad \phi' = 4(s_{\sqrt{y}})^2 - 1. \quad (2)$$

193 where  $(s_{\sqrt{y}})^2$  is the sample variance of  $\sqrt{y}$ , and thus

194 
$$(s_{\sqrt{y}})^2 = \frac{1}{n} \cdot \sum_{i=1}^n (\sqrt{y_i} - \overline{\sqrt{y}})^2 = \bar{y} - (\overline{\sqrt{y}})^2. \quad (3)$$

195 The square root transformation stabilizes the variance, i.e. removes the dependence between  
 196 mean and variance. Economou et al. (2015) showed that this also allows a regression of  $\sqrt{y}$  on  
 197 the NAO, in order to quantify the possible influence of the NAO on dispersion:

198 
$$\sqrt{y} = \alpha + \beta x + \varepsilon; \quad \varepsilon \sim N(0, \sigma^2) \quad (4)$$

199 where  $x$  is the seasonal mean of NAO. Parameters  $\alpha$  and  $\beta$  are estimated from the data, and  
 200 represent the intercept and slope parameters of the assumed linear relationship between  $\sqrt{y}$   
 201 and the NAO. The term  $\varepsilon$  represents the error about the straight line, and is assumed to follow  
 202 a Normal distribution with variance  $\sigma^2$ , which is also estimated from the data. To investigate  
 203 whether the assumption that NAO is linearly related to  $\sqrt{y}$  holds across all methods, we have  
 204 additionally implemented an extended regression assuming a quadratic relationship:

205 
$$\sqrt{y} = \alpha + \beta x + \gamma x^2 + \varepsilon; \quad \varepsilon \sim N(0, \sigma^2) \quad (5)$$

206 The estimated linear and quadratic relationships for two exemplary grid points near the Azores  
 207 and Iceland are shown in Figures S2 and S3. In general, these plots indicate that there is no  
 208 real difference between the linear and quadratic fits, so that the linear fit is retained. The NAO  
 209 index is calculated following the methodology by Barnston and Livezey (1987), which is  
 210 based on Rotated Principal Component Analysis. The monthly time series for December,  
 211 January and February were provided by the Climate Prediction Center from the National  
 212 Oceanic and Atmospheric Administration and averaged for each winter (DJF).

213 Using equation (4), it can be shown that

214 
$$\phi' = 4(s_{\sqrt{y}})^2 - 1 = 4\beta^2(s_x)^2 + 4\sigma^2 - 1 \quad (6)$$

215 where  $(s_x)^2$  is the sample variance of the NAO-index  $x$ . This allows to diagnose how much of  
216 the underdispersion can attributed to modulation of counts by NAO (the parameter  $\beta$ ).

### 217 218 **3. Quantification of cyclone passages on a grid point basis**

219 Time series of cyclone counts for all 15 methods are first analysed at each grid point. As an  
220 example, we consider the grid point 55°N, 5°W centered over the British Isles and cyclone  
221 counts for January 2007 (Fig. 1), a period characterized by a large number of storms over this  
222 area (Pinto et al., 2014). The corresponding 700 km identification radius is shown in Fig. 1b.  
223 The cyclone passages within this area are indicated in the time line (Fig. 1a) and show some  
224 similarities but also differences for the individual methods: for example, the number of  
225 identified cyclones for this grid point and month ranges from 5 (M22) to 25 (M18). On the  
226 other hand, the main cyclones passing through this area (9, 10, 12, 13, 15, 18 and 20 January;  
227 cf. Pinto et al., 2014; their Figure 3) are captured by most methods. Fig. 1b shows the  
228 individual tracks for all methods for the cyclone passing on 13 January (named storm “Hanno”  
229 by the Free University of Berlin). The tracks show generally a good agreement for all methods  
230 in the main development phase, when all tracks are found within a corridor of a few 100  
231 kilometers. Small differences between the tracks at this development stage are typical, given  
232 that the methods use different key variables for tracking: for example, the MLSP minima and  
233 850 hPa vorticity maxima do not exactly overlap in an extra-tropical cyclone (e.g. Pinto et al.,  
234 2005; their Figure 1), with the vorticity maxima (e.g., M07, M18, HOD) typically being  
235 located south of the former (e.g. M02, M06). Less agreement is found at the beginning  
236 (different starting points) and particularly at the end of the cyclone tracks, which show  
237 diverging trajectories over Eastern Europe: while most methods show a zonal track towards  
238 southern Finland and further into Northern Russia, some of the vorticity methods (green) show

239 a track towards the Caspian Sea. Similar results have been found in previous case studies  
240 analysed in the IMILAST project (Neu et al., 2013; their Figs 4 and 5).

241 Following this methodology, time series of cyclone counts are derived for each grid-point in  
242 the domain  $30^{\circ}\text{N} - 70^{\circ}\text{N}$  and  $80^{\circ}\text{W} - 20^{\circ}\text{E}$  and for the whole study period (winters 1979/80 to  
243 2009/10). The mean of counts  $\bar{y}$  and their variance  $(s_y)^2$ , the two components needed to  
244 estimate  $\phi$ , are displayed in Figures 2 and 3 for all 15 cyclone tracking methods. The number  
245 of tracks passing through a certain area ( $\bar{y}$ ; Figure 2) is comparable to a cyclone track density  
246 field, and depict higher magnitudes in areas with many transient cyclones. This is unlike  
247 cyclone count statistics, in which cyclones can be counted multiple times in the same location  
248 (cf. Pinto et al., 2005). Therefore, some intrinsic differences are found between Figure 2 and  
249 Figure 1 from Neu et al. (2013), which shows cyclone count statistics. This reveals a larger  
250 discrepancy between the algorithms compared to Neu et al. (2013), e.g. there is no common  
251 peak south of Greenland for all methods (Figure 2).

252 Differences between tracking methods are identified both in terms of total numbers, position  
253 of the North Atlantic storm track and regional aspects such as Mediterranean cyclones: For  
254 example, methods M14, M21 and M22 show generally small cyclone numbers and relatively  
255 weak activity over the Mediterranean Basin (Figure 2). This is not the case for other methods  
256 such as M02, M06, M15 and M20. However, the general spatial pattern in mean counts over  
257 the North Atlantic storm track qualitatively agrees between methods. Some of the spatial  
258 differences between methods can be explained by the choice of variable used in the tracking.  
259 For example, cyclone tracks based on 850 hPa vorticity (VORT) are typically displaced  
260 southwards to cyclone tracks derived from MSLP pressure minimum (cp. M15 and M18).

261 Systematic discrepancies between the various cyclone track algorithms also play a role for the  
262 identified differences. See also Neu et al. (2013) for more details. Specific differences within

263 the Mediterranean Basin are discussed in Lionello et al. (2016) and will not be further  
264 analysed here.

265 The variance of counts  $(s_y)^2$  shows more diverse results (Figure 3). Spatial patterns typically  
266 display a maximum of activity south of Greenland, which often extends towards Northern  
267 Europe. However, the relative maximum over Western / Central Europe is not found for some  
268 methods (e.g. M16, M21), or is displaced in others (M06, M18) to around 50°N–55°N over  
269 the Eastern North Atlantic. While this relative maximum is also found for other methods (e.g.  
270 M02, M15) it is not the dominant feature. In terms of numbers, the differences in  $(s_y)^2$   
271 between methods are even larger than for  $\bar{y}$ , with values differing by an order of magnitude in  
272 some areas, e.g. south of Greenland.

273

#### 274 **4. Quantification of clustering**

275 The estimates of  $\phi$  for the different methods are shown in Figure 4. The general spatial pattern  
276 qualitatively agrees between tracking methods, e.g. an area of  $\phi < 0$  identified over the western  
277 North Atlantic (regularity or underdispersion; blue colours), while  $\phi > 0$  (clustering or  
278 overdispersion; red colours) is found on northern and southern flanks and the downstream  
279 region of the North Atlantic storm track (cp. Mailier et al., 2006; Pinto et al., 2013).  
280 Considering the whole study area, overdispersion (red) tends to dominate for some methods  
281 (e.g., M15, M20), while underdispersion (blue) dominates for others (e.g., M21, M22).  
282 However, most methods show a balance between the two features (e.g. M02, M06, M18), in  
283 line with previous works (Mailier et al., 2006; Pinto et al., 2013). While all methods show  
284 overdispersion over Western Europe, the magnitude of  $\phi$  clearly differs between methods. For  
285 the example grid point 55°N, 5°W,  $\phi$  is positive for all methods (clustering), but ranges from  
286 0.27 (M21) to 4.73 (M20). Differences appear to be dominated primarily by the variance of  
287 winter counts (cf. Figure 3).

288 To provide further insight into the differences between methods, we analyse in detail the  
289 relations between  $\bar{y}$  and  $(s_y)^2$  for 55°N, 5°W. In Figure 5, the mean is plotted against the  
290 variance, and the lines corresponding to  $\phi = 0, 1, 2, 3, 4,$  and  $5$  are shown for orientation. Half  
291 of the methods are found in the range between  $\phi = 0.86$  and  $1.32$ , and four methods around  $2.0$   
292 (M07, M08, M09, M14). Methods M15, M20 and M21 are outliers: the two former methods  
293 (both based on MSLP) display a much higher  $(s_y)^2$  compared to  $\bar{y}$ , while for the latter  $(s_y)^2$   
294 and  $\bar{y}$  are small and roughly equal. The statistical significance bounds for the Poisson  
295 distribution ( $\phi = 0$ ) is estimated using parametric bootstrapping: 10000 time series of 30  
296 counts are generated for each mean value (1-55) assuming a Poisson distribution. For each  
297 mean value, the empirical 95% quantile of those 10000 variance values is used to construct a  
298 95% confidence interval (gray area around  $\phi = 0$  in Figure 5). This implies that dispersion  
299 values for all but two methods (M21, HOD) significantly deviate from Poisson. Similar results  
300 are found for other grid points over the Eastern North Atlantic and Western Europe (not  
301 shown), revealing the robustness of overdispersion of cyclone counts for this area.

302 The range of the horizontal axis (in Figure 5), which shows the mean, is much smaller than the  
303 range of the vertical axis, which shows the variance. This indicates that differences in  $(s_y)^2$   
304 are the primary driver behind the differences in  $\phi$ . For example,  $\bar{y}$  is actually quite similar for  
305 M20 and M21 (20.9 and 18.5, respectively), while  $(s_y)^2$  and thus  $\phi$  are very different. On the  
306 other hand, the consistency of results between M02 and M10 is noteworthy: these approaches  
307 basically use the same tracking method with different parameters, and provide very similar  
308 values of  $\phi$  (1.21 and 1.32) despite the differences in  $\bar{y}$ . Methods displaying underdispersion  
309 over most of the study area (e.g., M21, M22) typically have a small number of cyclone counts  
310 (cf. Fig. 2), but the dominant factor for the differences in  $\phi$  remains  $(s_y)^2$ . It is noteworthy  
311 that the two methods with the highest  $\phi$  values (M15, M20) are MSLP minimum methods

312 (orange/brown). However, other MSLP minimum methods (M12, M16) show values closer to  
313 the other approaches. It is therefore difficult to associate the diversity of  $\phi$  results with  
314 particular features of tracking methods. This result is consistent with the conclusions of Neu et  
315 al. (2013) and Rudeva et al. (2014) regarding cyclone characteristics and their possible  
316 dependence on the tracking method.

317

## 318 **5. Relationship with the NAO**

319 The recent study by Economou et al. (2015) showed that a considerable part of the  
320 overdispersion identified based on ERA-Interim reanalysis cyclone tracks derived with the  
321 HOD approach is due to the modulation of cyclone counts by the NAO. In order to investigate  
322 the NAO influence on cyclone clustering, dispersion is now quantified following Economou et  
323 al. (2015), where  $\phi$  is approximated by  $\phi' = 4(s_{\sqrt{y}})^2 - 1$  (equation 2). Results are shown in  
324 Figure 6 for each tracking method. The two estimation methods for  $\phi$  are very similar (cp.  
325 Figs 4 and 6), implying that the  $\phi'$  is a good approximation to  $\phi$ . In the following, we use this  
326 approximation to estimate the contribution of the NAO index to the dispersion index  
327 according to equation (6).

328 The linear relationship between the strength of the NAO  $x$  and  $\sqrt{y}$  is quantified by the  
329 parameter  $\beta$ . The result is a dipolar structure, revealing a positive pole near Iceland and a  
330 negative pole over the Azores (cf. Figure 7). This systematic influence of the NAO-Phase on  
331 clustering can now be quantified as  $4\beta^2(s_x)^2$  (equation 6). Figure 8 shows the NAO  
332 contribution for each method, revealing two maxima, one north and one south of the North  
333 Atlantic storm track. This general spatial pattern is in good agreement with Economou et al.  
334 (2015) who considered cyclone tracks derived with HOD method and ERA-40 data (Uppala et  
335 al., 2005). The North Atlantic storm track moves latitudinally depending on the NAO-phase,  
336 leading to the two maxima of NAO influence on clustering on the flanks of the storm track.



337 However, there are differences in the detail between the 15 methods, both in terms of spatial  
338 pattern and magnitude. This can be partly explained by the relationship between the NAO  
339 influence on dispersion and the magnitude of dispersion itself per method (compare Figures 4  
340 and 8). For example, a strong influence of the NAO on the clustering of cyclones is found in  
341 regions and methods where overdispersion is high (cp. Figure 4 and Figure 8 for M07, M08,  
342 M15, M20 near the Alps). The spatial pattern of NAO influence also shows some differences  
343 over Europe: for example, while the region with low NAO influence (white) is located over  
344 Northern Europe for most methods, a few methods have this region over Central Europe  
345 (M10, M18) or over France (M20). The spatial variability of the NAO-influence is high for  
346 some methods (M07, M08, M15), which indicates a larger uncertainty of the  $\beta$  estimate. In  
347 general, it is difficult to associate the different types of methods (e.g. using vorticity or MSLP  
348 as the cyclone tracking variable) with a specific type of behavior regarding the NAO influence  
349 on cyclone clustering over the North Atlantic and Europe, but the general agreement between  
350 the methods is encouraging.

351 The large differences in the number of counts between the methods leads to strong differences  
352 in  $\beta$  and therefore also on the absolute contribution of the NAO to overdispersion. As all the  
353 effects contributing to clustering can be quantified as  $4\beta^2(s_x)^2 + 4\sigma^2$  (equation 6), the  
354 relative contribution of the NAO is defined as  $4\beta^2(s_x)^2 / (4\beta^2(s_x)^2 + 4\sigma^2)$  and shown in  
355 Figure 9. A similar pattern to Figure 8 is revealed, with the two maxima near Iceland and the  
356 Azores, plus additional maxima over Central Europe or near Newfoundland. The relative  
357 contribution of the NAO to clustering exceeds 50% for some methods, particularly south of  
358 Iceland and in the region between Azores and Iberia. The intensity and extension of the area  
359 around each of the two maxima differ. For example, for M02, both maxima are approximately  
360 equally strong, while for M18 the southern maximum is more pronounced. This suggests a  
361 stronger (weaker) contribution of other processes than the NAO to the clustering for one

362 (other) maximum. Comparing the figures 3 and 9, it is quite apparent that there is no clear link  
363 between the difference in variance between methods and the sensitivity to the NAO.

364

## 365 **6. Conclusions**

366 The main objective of this paper was to assess if the cyclone clustering over the eastern North  
367 Atlantic and Europe is a robust feature using results from 15 cyclone tracking methods. A  
368 second objective was to evaluate whether the relationship between NAO and clustering  
369 depends on the choice of the tracking method. The main findings of this study are as follows:

370

- 371 • The general spatial pattern of the cyclone dispersion statistic ( $\phi$ ), as previously  
372 identified with single tracking methods, is qualitatively captured by all methods:  
373 underdispersion (regularity) is identified near the core of the North Atlantic storm  
374 track near Newfoundland, while overdispersion (clustering) can be found over the  
375 eastern North Atlantic and Western Europe, particularly on both sides and downstream  
376 of the North Atlantic storm track.
- 377 • Quantitative differences in the values of  $\phi$  are identified between methods. Some  
378 methods display predominantly underdispersion (regularity) over the study area,  
379 while others indicate overdispersion (clustering) over almost the whole study area.
- 380 • The differences in  $\phi$  can be primarily attributed to the differences in the variance of  
381 cyclone counts between the methods.
- 382 • Significant overdispersion is identified for almost all methods over parts of the Eastern  
383 North Atlantic and Western Europe, indicating the robustness of cyclone clustering in  
384 this area. Still, the magnitude of  $\phi$  may vary strongly between methods.
- 385 • The statistical link between NAO and clustering of cyclone tracks found for all  
386 methods and is thus a robust feature: in accordance with previous studies, maxima on

387 both sides of the main storm track are identified, though with slightly different  
388 magnitudes and spatial extension.

- 389 • The explained variance of the NAO on clustering exceeds 50% for some tracking  
390 methods and locations. The differences in the variance of cyclone counts cannot be  
391 attributed to different sensitivities to the NAO.

392

393 We conclude that both the general pattern of underdispersion / overdispersion over the North  
394 Atlantic and Western Europe and the dipolar pattern of NAO influence on dispersion are  
395 largely independent from the choice of tracking method and hence from the definition of a  
396 cyclone. In particular, overdispersion of cyclone counts is identified for all methods over the  
397 Western Europe, and can therefore be considered as a robust feature. This is important and  
398 valuable information for stakeholders, such as the insurance industry, for whom the clustering  
399 of extreme cyclones is a major economic risk.

400 The present results suggest that estimates of cyclone clustering obtained with single tracking  
401 methods can be regarded as qualitatively representative for a wider range of tracking methods.  
402 This is particularly important because cyclone clustering may change under future climate  
403 conditions (Pinto et al., 2013). Given the large sampling uncertainty, such potential changes  
404 may not be detectable in single 30-year climate model simulations (Economou et al., 2015).  
405 Still, Karremann et al. (2014) has recently provided evidence based on a large ensemble of  
406 simulations with a single global circulation model that cumulative annual losses associated  
407 with extra-tropical cyclones may increase over most of Europe in future decades due to a  
408 combination of changes in potential loss magnitude and changes in storm clustering.

409 Future research could analyse differences between tracking methods also in higher resolution  
410 reanalysis datasets such as NASA-MERRA (Rienecker et al., 2011). The higher spatial and  
411 temporal resolution will permit a better quantification of the features identified here and a

412 more detailed dynamical analysis similar to Pinto et al. (2014). Another interesting line of  
413 research is to quantify the role of the jet location and intensity for cyclone clustering across  
414 Western Europe. Preliminary results (for the grid point 55°N, 5°W) indicate that winters with  
415 a stronger jet also have a higher number of counts for all methods, particularly when the jet is  
416 located around 45°N-50°N (not shown). Finally, it will be interesting to investigate clustering  
417 of extratropical cyclones in global circulation models in more detail, taking into account how  
418 cyclones and cyclone clustering are represented at different resolutions, evaluating the  
419 representation of the associated physical processes, and analysing how results depend on the  
420 tracking method.

421

## 422 **Acknowledgements**

423 The authors would like to thank Swiss Re for sponsoring the Intercomparison of Mid-Latitude  
424 Storm Diagnostics (IMILAST) project. T.E. and D.B.S. were supported by NERC project  
425 CREDIBLE. We thank the European Center of Medium Range Weather Forecast (ECMWF,  
426 [www.ecmwf.int](http://www.ecmwf.int)) for the ERA-Interim reanalysis, and the Climate Prediction Center from the  
427 National Oceanic and Atmospheric Administration for the NAO index  
428 (<http://www.cpc.ncep.noaa.gov/products/precip/CWlink/pna/nao.shtml>). We thank all the  
429 members of the IMILAST project ([www.proclim.ch/imilast](http://www.proclim.ch/imilast)) for making the cyclone tracks  
430 available. We also thank Kevin Hodges for making the cyclone tracks available for this study  
431 and for discussions. The present manuscript profited from discussion with various members of  
432 the IMILAST project group. We are thankful to the two anonymous reviewers for their  
433 valuable comments and suggestions on a previous version of this manuscript.

434

435 **References**

- 436 Akperov, M. G., Bardin, M. Y., Volodin, E. M., Golitsyn, G. S. and Mokhov, I. I. 2007.  
437 Probability distributions for cyclones and anticyclones from the NCEP/NCAR reanalysis  
438 data and the INM RAS climate model. *Izvest. Atmos. Ocean. Phys.* **43**, 705-712. doi:  
439 10.1134/S0001433807060047.
- 440 Bardin, M. Y. and Polonsky, A. B. 2005. North Atlantic Oscillation and synoptic variability in  
441 the European-Atlantic region in winter. *Izvest. Atmos. Ocean. Phys.* **41**, 127-136.
- 442 Barnston, A. G., and Livezey, R. E. 1987. Classification, seasonality and persistence of low-  
443 frequency atmospheric circulation patterns. *Mon. Weather Rev.* **115**, 1083–1126. doi:  
444 10.1175/1520-0493(1987)115<1083:CSAPOL>2.0.CO;2.
- 445 Blender, R., Fraedrich, K., and Lunkeit, F. 1997. Identification of cyclone track regimes in the  
446 North Atlantic. *Q. J. Roy. Meteorol. Soc.* **123**, 727-741. doi: 10.1002/qj.49712353910.
- 447 Blender R., Raible, C.C., and Lunkeit, F. 2015. Non-exponential return time distributions for  
448 vorticity extremes explained by fractional Poisson processes. *Q. J. Roy. Meteorol. Soc.* **141**,  
449 249–257. doi: 10.1002/qj.2354.
- 450 Bjerknes, J., and Solberg, H. 1922. Life cycle of cyclones and the polar front theory of  
451 atmospheric circulation, *Geofys. Publ.* **3**, 3–18.
- 452 Cox, D. R., and Isham, V. 1980. Point Processes, pp. 188, Chapman and Hall/CRC, London.
- 453 Dee, D. P., Uppala, S. M., Simmons, A. J., Berrisford, P., Poli, P., and co-authors. 2011. The  
454 ERA-Interim reanalysis: Configuration and performance of the data assimilation system. *Q.*  
455 *J. Roy. Meteorol. Soc.* **137**, 553–597. doi: 10.1002/qj.828.
- 456 Economou, T., Stephenson, D. B., Ferro, C. A. T. 2014. Spatio-temporal modelling of extreme  
457 storms. *Ann. Appl. Stat.* **8**, 2223-2246. doi:10.1214/14-AOAS766.

458 Economou, T., Stephenson, D. B., Pinto, J. G., Shaffrey, L. C., Zappa, G. 2015. Serial  
459 clustering of extratropical cyclones in historical and future CMIP5 model simulations. *Q. J.*  
460 *Roy. Meteorol. Soc.* **141**, 3076–3087. doi: 10.1002/qj.2591.

461 Flaounas, E., Kotroni, V., Lagouvardos, K. and Flaounas, I. 2014. CycloTRACK (v1.0):  
462 Tracking winter extratropical cyclones based on relative vorticity: Sensitivity to data  
463 filtering and other relevant parameters. *Geosci. Model Dev.* **7**, 1841-1853. doi:  
464 10.5194/gmd-7-1841-2014.

465 Gómara, I., Pinto, J. G., Woollings, T., Masato, G., Zurita-Gotor, P. and Rodríguez-Fonseca,  
466 B. 2014. Rossby wave-breaking analysis of explosive cyclones in the Euro-Atlantic sector,  
467 *Q. J. Roy. Meteorol. Soc.* **140**, 738–753. doi: 10.1002/qj.2190.

468 Hanley, J., and Caballero, R. 2012. The role of large-scale atmospheric flow and Rossby wave  
469 breaking in the evolution of extreme windstorms over Europe. *Geophys. Res. Lett.* **39**,  
470 L21708. doi: 10.1029/2012GL053408.

471 Hewson, T. D. 1997. Objective identification of frontal wave cyclones. *Meteorol. Appl.* **4**,  
472 311-315. doi: 10.1017/S135048279700073X.

473 Hewson, T. D. and Tittley, H. A. 2010. Objective identification, typing and tracking of the  
474 complete lifecycles of cyclonic features at high spatial resolution. *Meteorol. Appl.* **17**, 355-  
475 381. doi: 10.1002/met.204.

476 Hewson, T. D. and Neu, U. 2015. Cyclones, windstorms and the IMILAST project. *Tellus A*  
477 **67**, 27128, doi: 10.3402/tellusa.v67.27128

478 Hodges, K. I. 1994. A general method for tracking analysis and its application to  
479 meteorological data. *Mon. Weather Rev.* **122**, 2573–2585. doi: 10.1175/1520-  
480 0493(1994)122<2573:AGMFTA>2.0.CO;2.

481 Hodges, K. I. 1999. Adaptive constraints for feature tracking. *Mon. Weather Rev.* **127**, 1362–  
482 1373. doi: 10.1175/1520-0493(1999)127<1362:ACFFT>2.0.CO;2.

483 Hodges, K. I., Lee, R. W., and Bengtsson, L. 2011. A comparison of extratropical cyclones in  
484 recent reanalyses ERA-Interim, NASA MERRA, NCEP CFSR, and JRA-25. *J. Clim.* **24**,  
485 4888–4906. doi: 10.1175/2011JCLI4097.1.

486 Hoskins, B. J. and Hodges, K. I. 2002. New perspectives on the Northern Hemisphere winter  
487 storm tracks. *J. Atmos. Sci.*, **59**, 1041-1061. doi: 10.1175/1520-  
488 0469(2002)059<1041:NPOTNH>2.0.CO;2.

489 Hunter, A., Stephenson, D.B., Economou, T., Holland, M. and Cook, I. 2016. New  
490 perspectives on the aggregated risk of extratropical cyclones. *Q. J. Roy. Meteorol. Soc.* **142**,  
491 243–256. doi:10.1002/qj.2649.

492 Huntingford, C., Marsh, T., Scaife, A. A., Kendon, E. J., Hannaford, J. and co-authors 2014.  
493 Potential influences in the United Kingdom's floods of winter 2013–2014. *Nat. Clim.*  
494 *Change* **4**, 769–777. doi: 10.1038/nclimate2314.

495 Hurrell, J. W., Kushnir, Y., Ottersen, G. and Visbeck, M. 2003. An Overview of the North  
496 Atlantic Oscillation, in *The North Atlantic Oscillation: Climatic Significance and*  
497 *Environmental Impact* (eds J. W. Hurrell, Y. Kushnir, G. Ottersen and M. Visbeck),  
498 American Geophysical Union, Washington, D. C. doi: 10.1029/134GM01.

499 Inatsu, M., 2009: The neighbor enclosed area tracking algorithm for extratropical wintertime  
500 cyclones. *Atmos. Sci. Lett.* **10**, 267-272. doi: 10.1002/asl.238.

501 Karremann, M. K., Pinto, J. G., Reyers, M., Klawa, M. 2014. Return periods of losses  
502 associated with European windstorm series in a changing climate. *Environ. Res. Lett.* **9**,  
503 124016. doi: 10.1088/1748-9326/9/12/124016.

504 Kew, S. F., Sprenger, M. and Davies, H. C. 2010. Potential vorticity anomalies of the  
505 lowermost stratosphere: A 10-yr winter climatology. *Mon. Weather Rev.* **138**, 1234-1249.  
506 doi: 10.1175/2009MWR3193.1.

507 Lionello, P., Dalan, F. and Elvini, E. 2002. Cyclones in the Mediterranean region: The present  
508 and the doubled CO2 climate scenarios. *Clim. Res.* **22**, 147-159. doi: 10.3354/cr022147.

509 Lionello, P., Trigo, I. F., Gil, V., Liberato, M. L. R., Nissen, K. M., and co-authors. 2016.  
510 Objective Climatology of Cyclones in the Mediterranean Region: a consensus view among  
511 methods with different system identification and tracking criteria. *Tellus A*, **68**, 29391. doi:  
512 10.3402/tellusa.v68.29391

513 Mailier, P. J., Stephenson, D. B., Ferro, C. A. T., and Hodges, K. I. 2006. Serial clustering of  
514 extratropical cyclones. *Mon. Weather Rev.* **134**, 2224-2240. doi: 10.1175/MWR3160.1.

515 Matthews, T., Murpy, C., Wilby, R. L., and Harrigan, S. 2014. Stormiest winter on record for  
516 Ireland and UK. *Nat. Clim. Change* **4**, 738–740. doi: 10.1038/nclimate2336.

517 Messori, G., and Caballero, R. 2015. On double Rossby wave breaking in the North Atlantic.  
518 *J. Geophys. Res. Atmos.* **120**, 11129–11150. doi: 10.1002/2015JD023854.

519 Murray, R. J. and Simmonds, I. 1991. A numerical scheme for tracking cyclone centres from  
520 digital data. Part I: Development and operation of the scheme. *Aust. Meteorol. Mag.* **39**,  
521 155-166.

522 Neu, U., Akperov, M. G., Bellenbaum, N., Benestad, R., Blender, R., and co-authors. 2013.  
523 IMILAST - a community effort to intercompare extratropical cyclone detection and  
524 tracking algorithms: assessing method-related uncertainties. *Bull. Am. Meteorol. Soc.* **94**,  
525 529-547. doi: 10.1175/BAMS-D-11-00154.1.

526 Parker, D. J. 1998. Secondary frontal waves in the North Atlantic region: A dynamical  
527 perspective of current ideas. *Q. J. Roy. Meteorol. Soc.* **124**, 829–856.  
528 doi: 10.1002/qj.49712454709.

529 Pinto, J. G., Spanghel, T., Ulbrich, U. and Speth, P. 2005. Sensitivities of a cyclone detection  
530 and tracking algorithm: Individual tracks and climatology. *Meteorol. Z.* **14**, 823-838. doi:  
531 10.1127/0941-2948/2005/0068.



532 Pinto, J. G., and Raible C. C. 2012. Past and recent changes in the North Atlantic oscillation.  
533 *Wiley Interdisc. Rev. Clim. Change* **3**, 79–90. doi: 10.1002/wcc.150.

534 Pinto, J. G., Bellenbaum, N., Karremann, M. K., and Della-Marta, P. M. 2013. Serial  
535 clustering of extratropical cyclones over the North Atlantic and Europe under recent and  
536 future climate conditions, *J. Geophys. Res. Atmos.*, **118**, 12476–12485. doi:  
537 10.1002/2013JD020564.

538 Pinto, J. G., Gómara, I., Masato, G., Dacre, H. F., Woollings, T., Caballero, R. 2014. Large-  
539 scale dynamics associated with clustering of extra-tropical cyclones affecting Western  
540 Europe. *J. Geophys. Res. Atmos.*, **119**, 13704–13719. doi: 10.1002/2014JD022305.

541 Raible, C. C., Della-Marta, P., Schwierz, C., Wernli, H., and Blender, R., 2008. Northern  
542 Hemisphere extratropical cyclones: A comparison of detection and tracking methods and  
543 different reanalyses. *Mon. Weather Rev.* **136**, 880-897. doi: 10.1175/2007MWR2143.1.

544 Rienecker, M. M., Suarez M. J., Gelaro R., Todling, R., Bacmeister J., and Coauthors. 2011.  
545 MERRA: NASA's Modern-Era Retrospective Analysis for Research and Applications. *J.*  
546 *Clim.* **24**, 3624–3648. doi: 10.1175/JCLI-D-11-00015.1.

547 Rudeva, I., and Gulev, S.K. 2007. Climatology of cyclone size characteristics and their  
548 changes during the cyclone life cycle. *Mon. Weather Rev.* **135**, 2568–2587. doi:  
549 10.1175/MWR3420.1.

550 Rudeva, I., Gulev, S. K., Simmonds, I., and Tilinina, N. 2014. The sensitivity of  
551 characteristics of cyclone activity to identification procedures in tracking algorithms. *Tellus*  
552 *A*, **66**, 24961. doi: 10.3402/tellusa.v66.24961.

553 Serreze, M. C. 1995. Climatological aspects of cyclone development and decay in the Arctic.  
554 *Atmos.-Ocean* **33**, 1-23. doi: 10.1080/07055900.1995.9649522

555 Simmonds, I., Keay, K. and Lim, E.-P. 2003. Synoptic activity in the seas around Antarctica.  
556 *Mon. Weather Rev.* **131**, 272-288. doi: 10.1175/1520-  
557 0493(2003)131<0272:SAITSA>2.0.CO;2.

558 Sinclair, M. R., 1994. An objective cyclone climatology for the Southern Hemisphere. *Mon.*  
559 *Wea. Rev.* **122**, 2239-2256. doi: 10.1175/1520-0493(1994)122<2239:AOCCT>2.0.CO;2.

560 Sinclair, M. R. 1997. Objective identification of cyclones and their circulation intensity, and  
561 climatology. *Weather Forecast.* **12**, 595-612. doi: 10.1175/1520-  
562 0434(1997)012<0595:OIOCAT>2.0.CO;2.

563 Trigo, I. F. 2006. Climatology and interannual variability of storm-tracks in the Euro-Atlantic  
564 sector: a comparison between ERA-40 and NCEP/NCAR reanalyses. *Clim. Dyn.* **26**, 127–  
565 143. doi: 10.1007/s00382-005-0065-9.

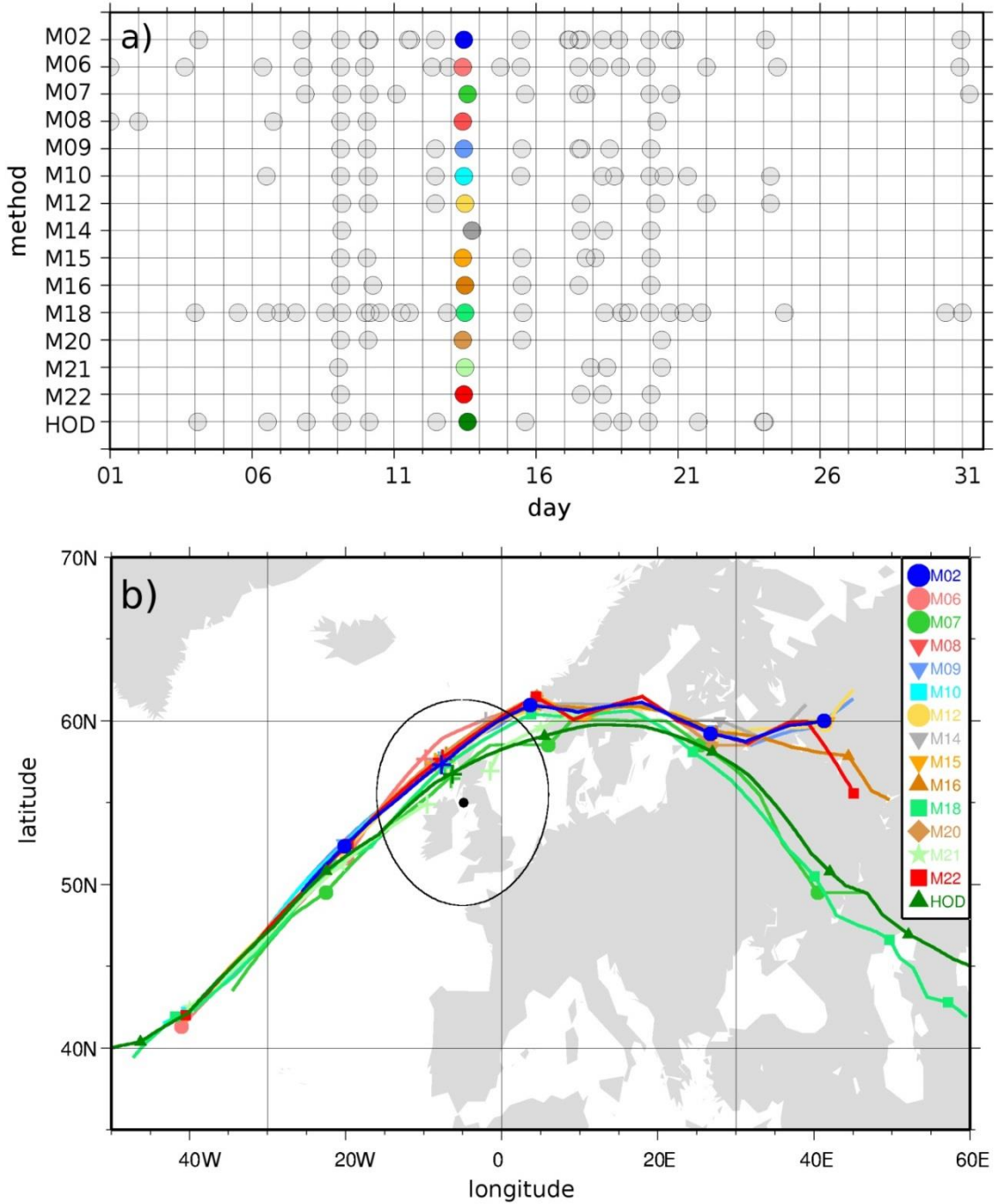
566 Uppala, S. M., Källberg, P. W., Simmons, A. J., Andrae, U., Bechtold, V. D. C., and co-  
567 authors. 2005. The ERA-40 re-analysis. *Q. J. Roy. Meteorol. Soc.* **131**, 2961–3012.  
568 doi: 10.1256/qj.04.176.

569 Vitolo, R., Stephenson, D. B., Cook, I. M., and Mitchell-Wallace, K. 2009. Serial clustering of  
570 intense European storms. *Meteorol. Z.*, **18**, 411-424. doi: 10.1127/0941-2948/2009/0393

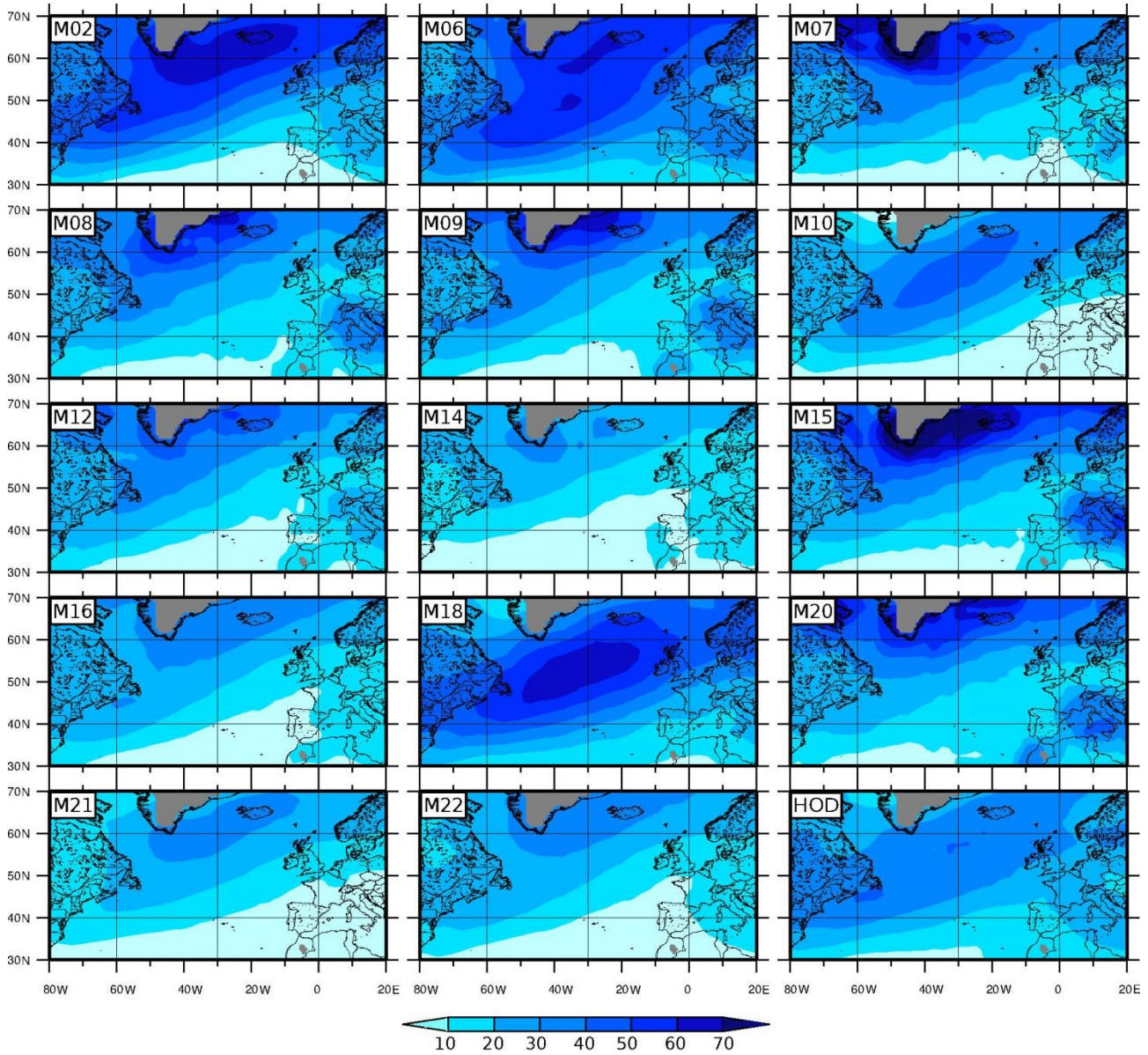
571 Wang, X. L., Swail, V. R. and Zwiers, F. W. 2006. Climatology and changes of extratropical  
572 cyclone activity: Comparison of ERA-40 with NCEP-NCAR reanalysis for 1958-2001. *J.*  
573 *Clim.* **19**, 3145-3166. doi: 10.1175/JCLI3781.1.

574 Wernli, H. and Schwierz, C. 2006. Surface cyclones in the ERA-40 dataset (1958-2001). Part  
575 I: Novel identification method and global climatology. *J. Atmos. Sci.* **63**, 2486-2507. doi:  
576 10.1175/JAS3766.1.

577 Zolina, O. and Gulev, S. K. 2002. Improving the accuracy of mapping cyclone numbers and  
578 frequencies. *Mon. Weather Rev.* **130**, 748-759. doi: 10.1175/1520-  
579 0493(2002)130<0748:ITAOMC>2.0.CO;2.



582 **Figure 1:** (a) Cyclone count time series of cyclone passages in January 2007 for different  
 583 methods (M02-M22, cf Table 1) for the grid point 55°N, 5°W (black dot in b). Events on  
 584 January 13th are marked in colour for each method. (b) Map with tracks corresponding to  
 585 marked events in a). Closest position of the track to the grid point is marked by +.  
 586

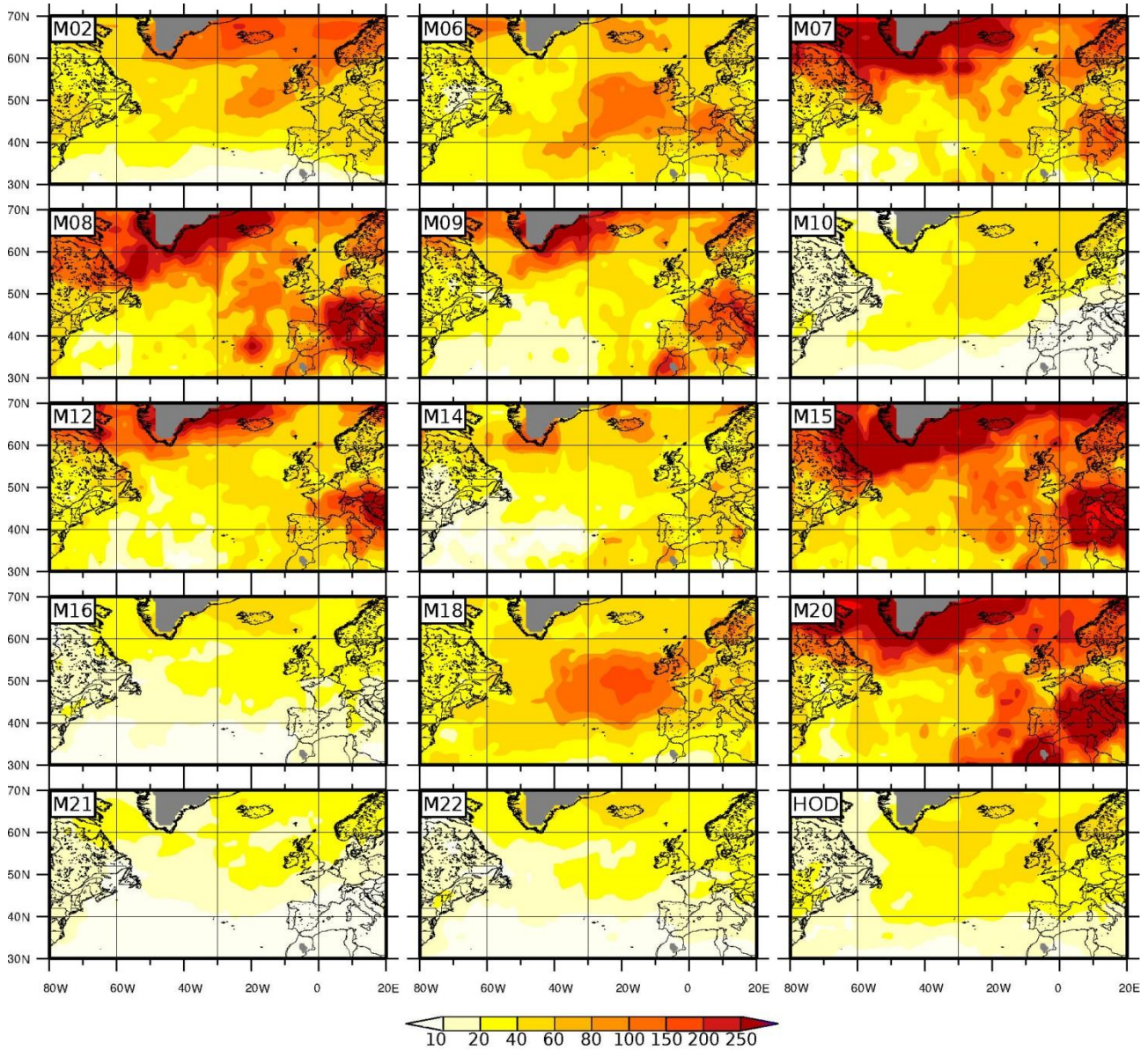


589  
590

591 **Figure 2:** Average number of DJF cyclone passages  $\bar{y}$  for each of the 15 methods (M02-M22,

592 HOD) derived from ERA-Interim (1979-2010).

593  
594  
595  
596



597  
598

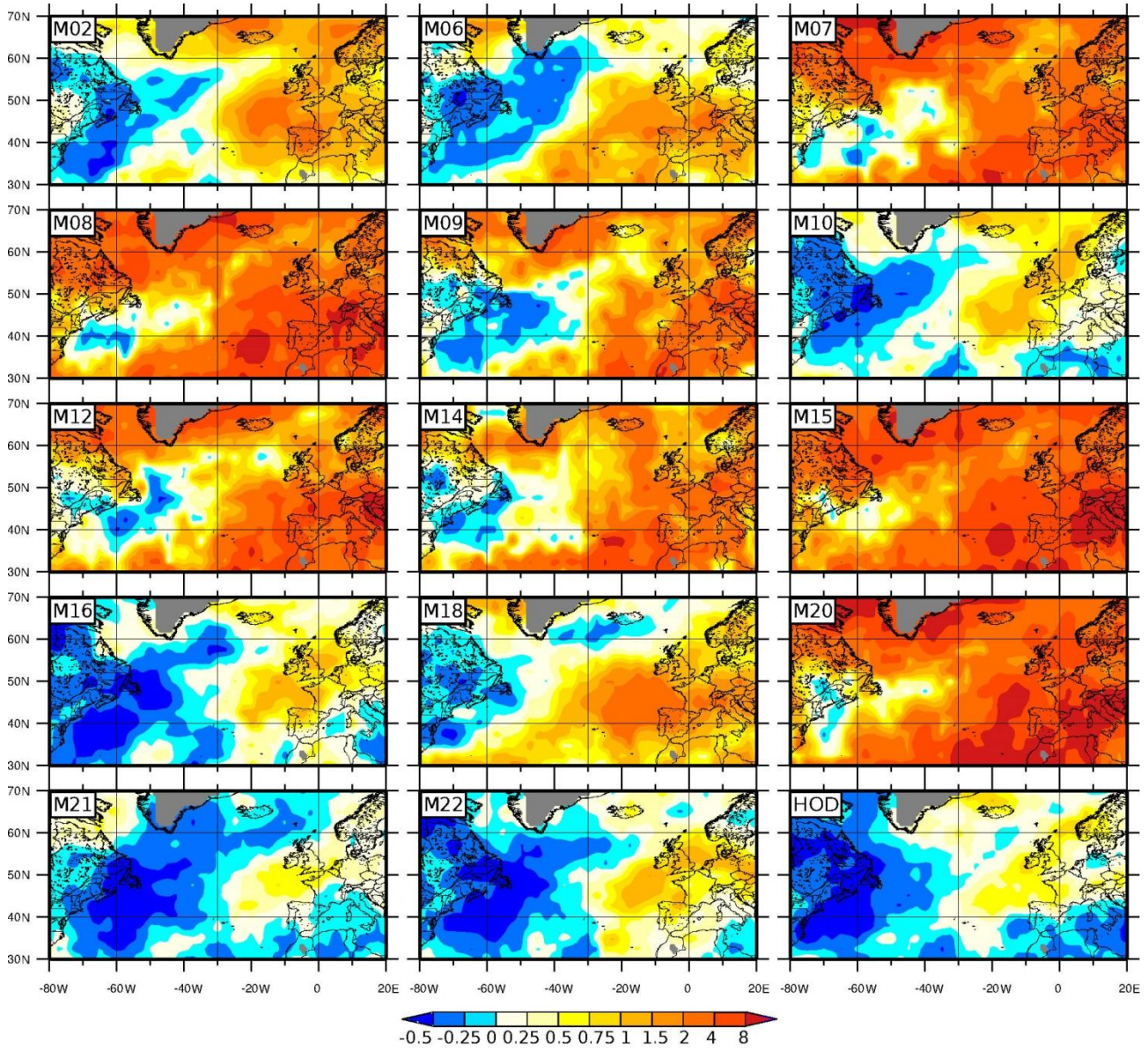
599 **Figure 3** Variance of DJF cyclone passages  $(s_y)^2$  for each of the 15 methods (M02-M22,

600 HOD) derived from ERA-Interim (1979-2010).

601

602

603



604

605

606 **Figure 4:** Dispersion statistic  $\phi$  for each of the 15 methods (M02-M22, HOD) derived from

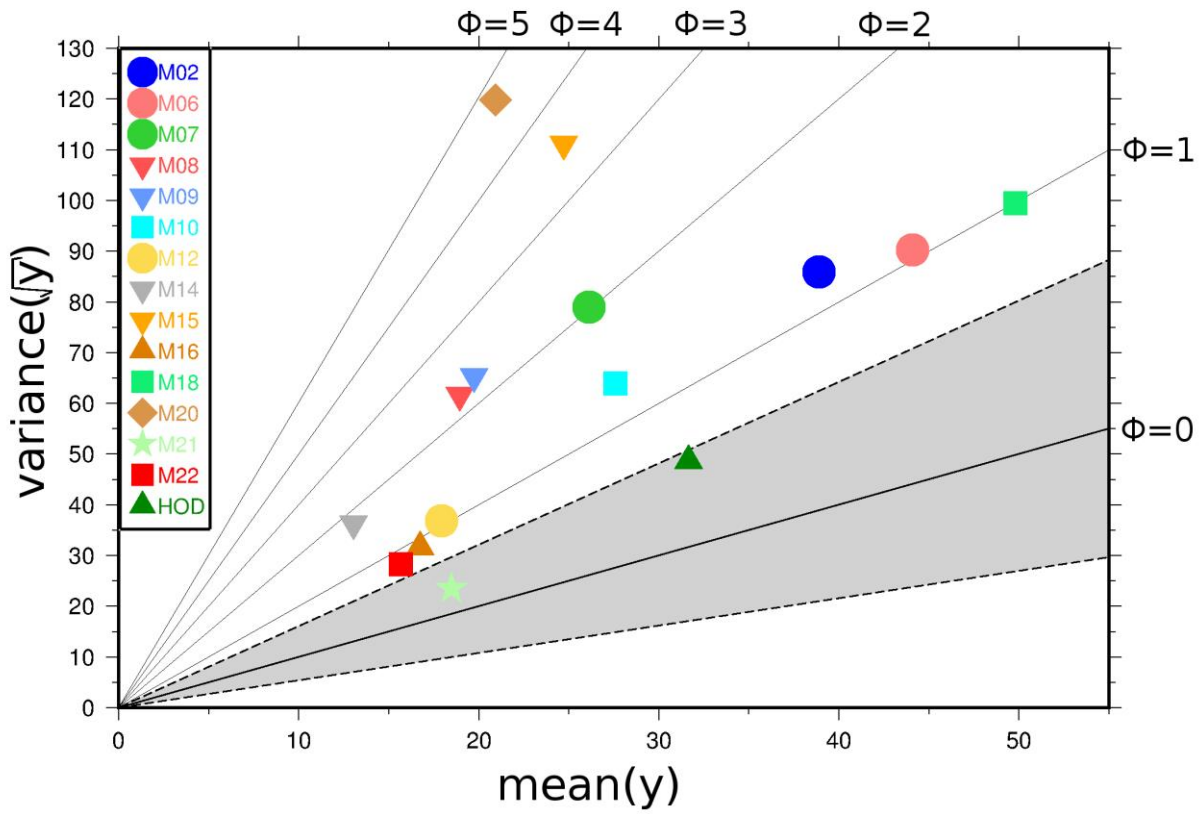
607 ERA-Interim (1979-2010).

608

609

610

611



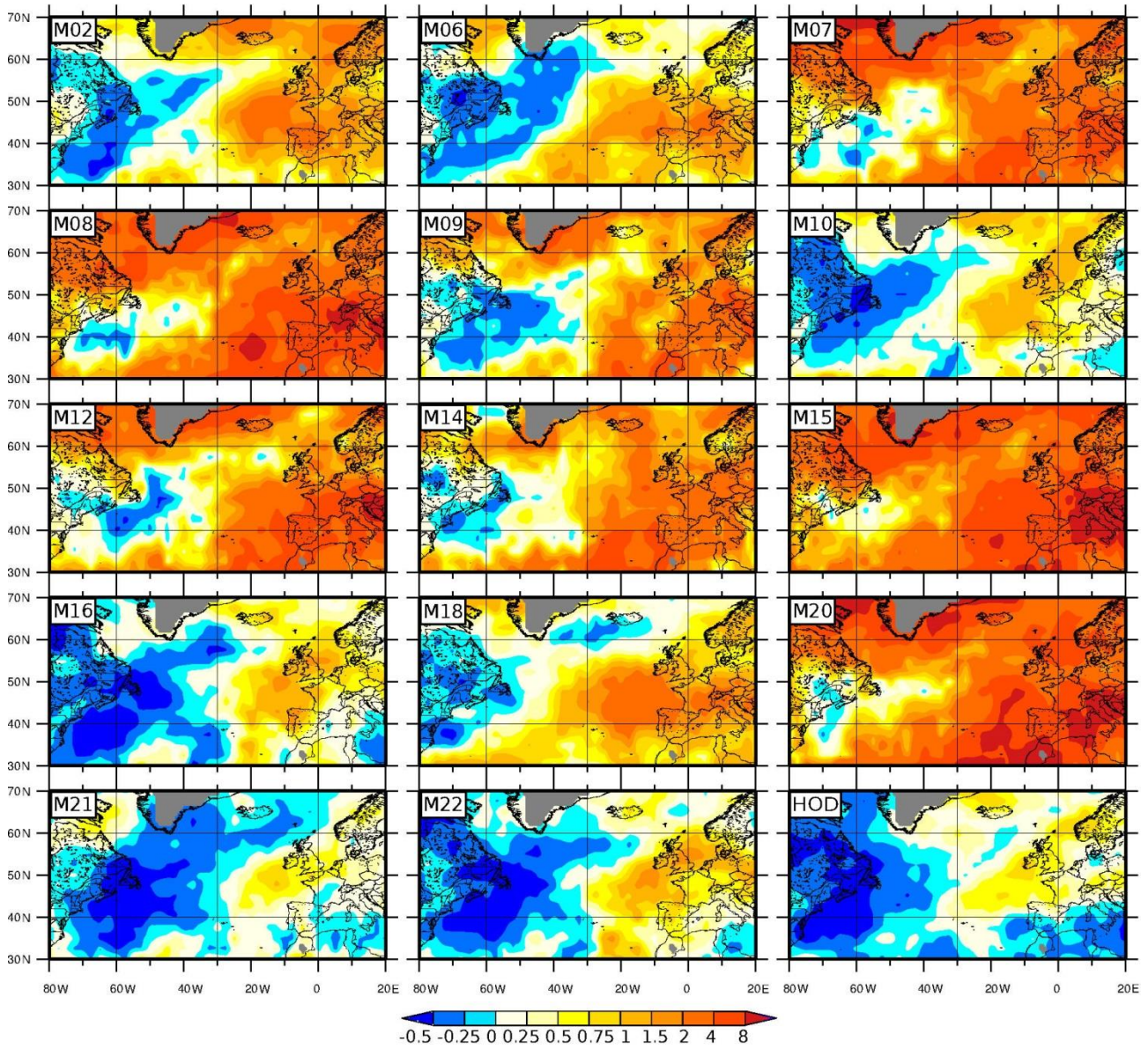
612

613

614 **Figure 5:** Variance  $(s_{\sqrt{\bar{y}}})^2$  (y-axis) and mean of cyclone track counts per winter  $\bar{y}$  (x-axis) for  
 615 the grid point 55°N, 5°W for each method (M02-M22,HOD). Isolines of dispersion statistic  $\phi$   
 616 are depicted in black (for values 0 to 5). The gray area depicts a 95% (bootstrap) confidence  
 617 interval for the variance, under the assumption of no overdispersion.

618

619

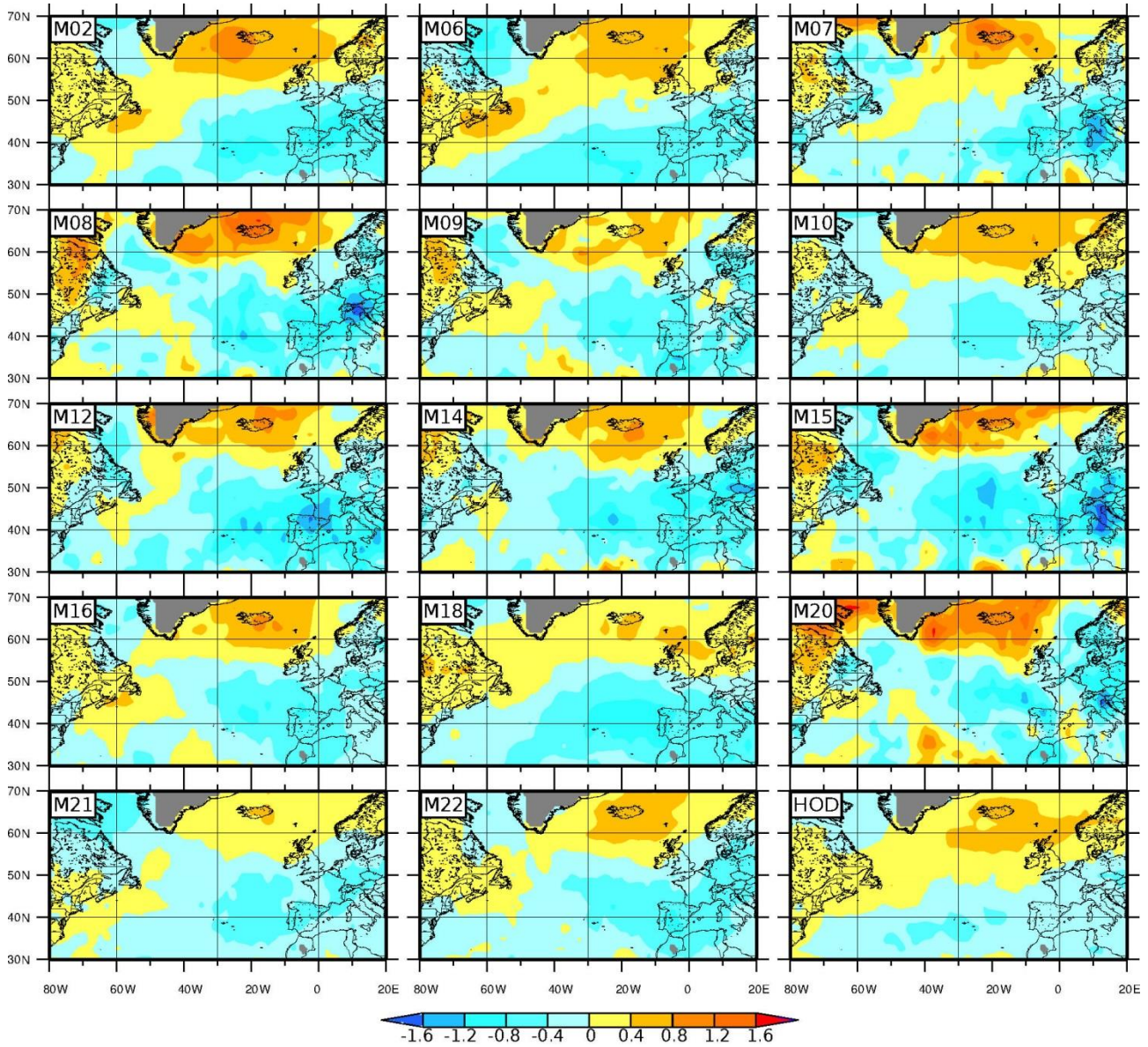


620  
621

622 **Figure 6:** Estimated dispersion statistic  $\phi'$  quantified with  $4 \cdot (s_{\sqrt{y}})^2 - 1$  for each of the 15  
623 methods (M02-M22, HOD) derived from ERA-Interim (1979-2010).

624  
625

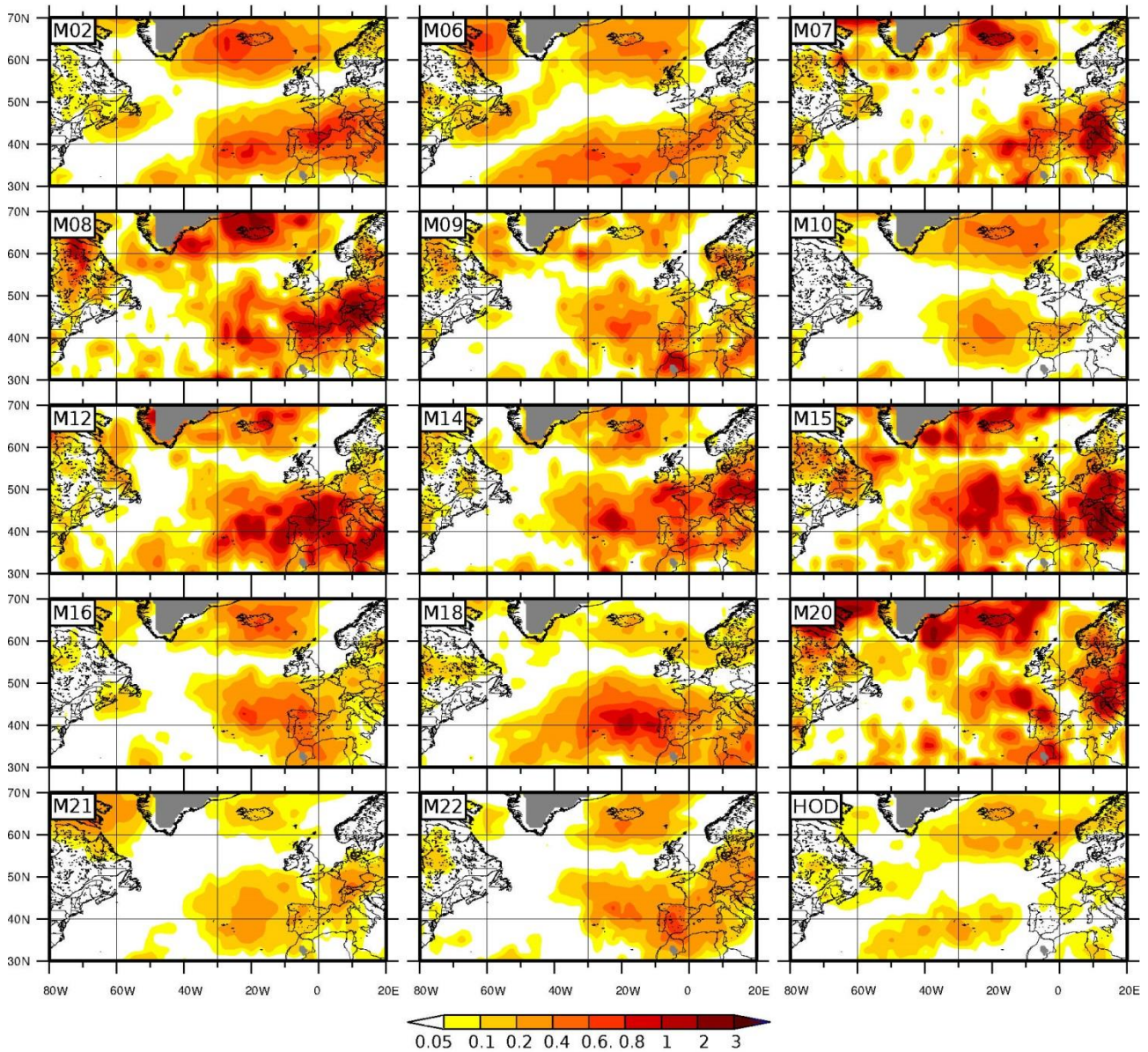




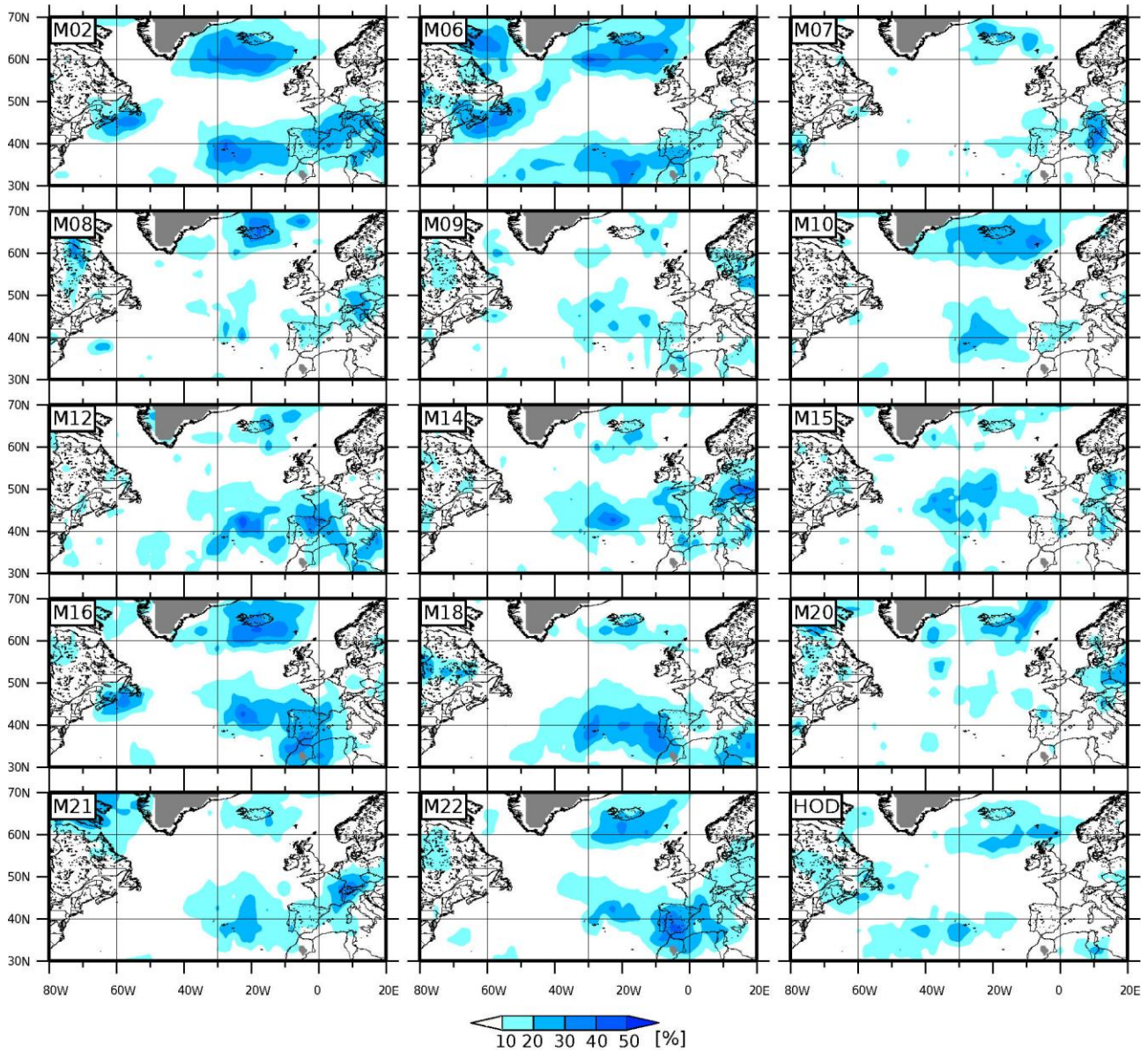
626  
627

628 **Figure 7:** Regression coefficient  $\beta$  (see EQ.3) for each of the 15 methods (M02-M22, HOD)

629 derived from ERA-Interim (1979-2010).



630 **Figure 8:** Effect of NAO on dispersion following  $4\beta^2(s_x)^2$  for each of the 15 methods (M02-  
 631 M22, HOD) derived from ERA-Interim (1979-2010).  
 632  
 633



634

635 **Figure 9:** Relative effect of NAO on dispersion following  $\beta^2(s_x)^2/(s_{\sqrt{y}})^2$  for each of the 15

636 methods (M02-M22, HOD) derived from ERA-Interim (1979-2010).

637

638

639

640 **Table 1:** List of cyclone tracking methods used in this study according to the IMILAST  
641 project denominations (Code M02-M22, HOD), main references of the method description,  
642 and main variable used (MSLP: mean sea level pressure; VORT: vorticity or Laplacian of  
643 MSLP; Z850 VORT: vorticity at 850 hPa; Z850: geopotential height at 850 hPa; grad.:  
644 gradient of MSLP; min: minimum).

645

Code	Main references for method description	Main variable used
M02	Murray and Simmonds (1991), Pinto et al. (2005)	MSLP (min), VORT
M06	Hewson (1997), Hewson and Titley (2010)	MSLP (min. grad.)
M07	Flaounas et al. (2014)	Z850 VORT
M08	Trigo (2006)	MSLP (min. grad.)
M09	Serreze (1995), Wang et al. (2006)	MSLP (min. grad.), VORT
M10	Murray and Simmonds (1991), Simmonds et al. (2003)	MSLP (min), VORT
M12	Zolina and Gulev (2002), Rudeva and Gulev (2007)	MSLP (min)
M14	Kew et al. (2010)	Z850 (min. contour)
M15	Blender et al. (1997), Raible et al. (2008)	MSLP (min)
M16	Lionello et al. (2002)	MSLP (min)
M18	Sinclair (1994, 1997)	Z850 VORT
M20	Wernli and Schwierz (2006)	MSLP (min)
M21	Inatsu (2009)	Z850 VORT
M22	Bardin and Polonsky (2005), Akperov et al. (2007)	MSLP (min. contour)
HOD	Hodges (1994), Hodges (1999), Hodges et al. (2011)	Z850 VORT

646

647

648 **Supplementary Material**

649

650

Randomness, Poisson process ( $\Phi=0$ )



Regularity, underdispersion ( $\Phi<0$ )



Clustering, overdispersion ( $\Phi>0$ )



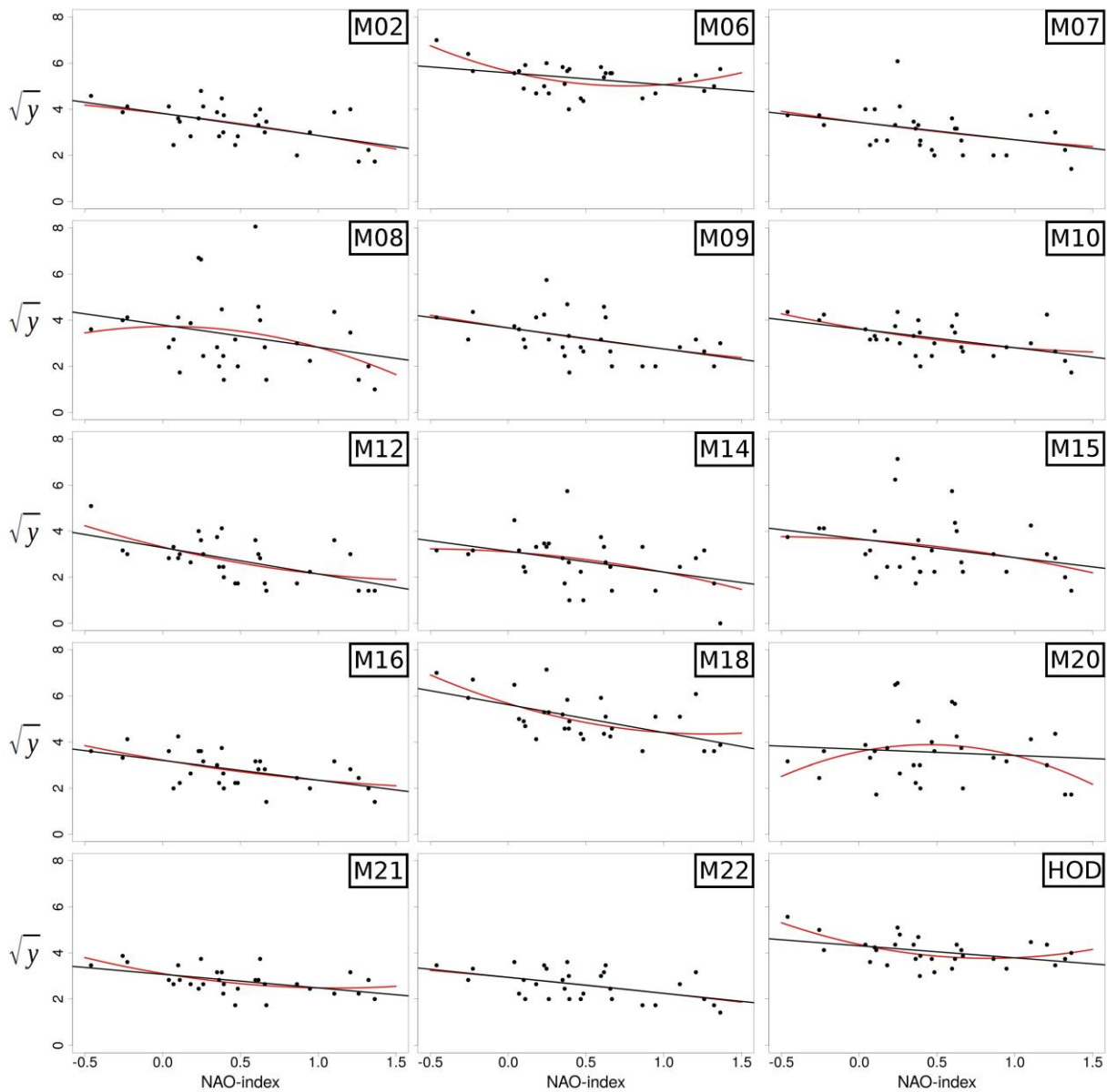
651

652 **Figure S1:** Examples of time series with randomness, regularity and clustering of counts. For

653 more details see text.

654

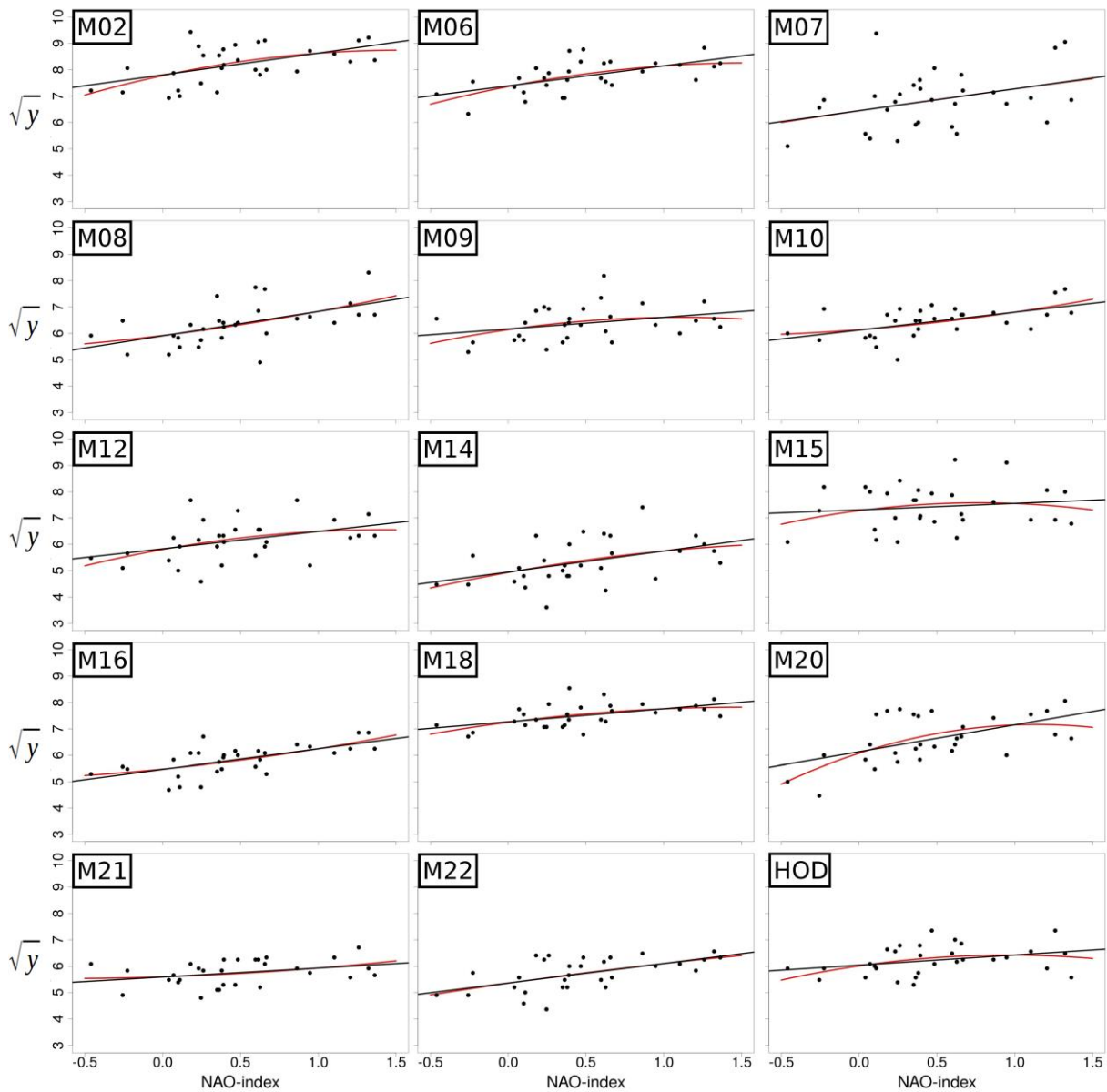
655



656  
657

658 **Figure S2:** Scatter plot of NAO index and  $\sqrt{y}$  of the grid point 40°N, 20°W for each of the 15  
 659 methods (M02-M22, HOD) derived from ERA-Interim (1979-2010) including the linear  
 660 (black line) and the quadratic (red line) fits.

661



662  
663

664 **Figure S3:** Scatter plot of NAO index and  $\sqrt{y}$  of the grid point 62.5°N, 20°W for each of the  
 665 15 methods (M02-M22, HOD) derived from ERA-Interim (1979-2010) including the linear  
 666 (black line) and the quadratic (red line) fits.

667  
668